Percolation, sliding, localization and relaxation in topologically closed circuits

Daniel Hurowitz, Doron Cohen

Department of Physics, Ben-Gurion University of the Negev, Beer-Sheva, Israel

The "glassy" version of *random walk on disordered lattice* features a percolation-related crossover to variable-range-hopping, or to sub-diffusion in one-dimension. The more general problem of *random walk in random environment*, where transition rates are allowed to be asymmetric, has been explored by Sinai, Derrida, and followers. It turns out that for any small amount of disorder an unbiased spreading in one-dimension becomes sub-diffusive, while for bias that exceeds a finite threshold there is a *sliding transition*, leading to a non-zero drift velocity. In the present study we explore the implications of the percolation and sliding transitions for the relaxation modes of a topologically closed circuit. A complementary question regarding the "delocalization" of eigenstates of non-hermitian Hamiltonians has been addressed by Hatano, Nelson, and followers. But we show that for a conservative random-walk dynamics the implied spectral properties are dramatically different.

It is essential to make a distinction between different versions of Einstein's Brownian motion problem. The original version is like analyzing a simple *random walk*. The resistor-network percolation problem [1], is like analyzing *random walk on a disordered lattice*, and has diverse applications, e.g. in the context of "glassy" electron dynamics [2, 3]. But more generally we have to consider Sinai's spreading problem [4–7], aka *random walk in a random environment*, that has relevance for studies in a biophysical context: pulling pinned polymers, DNA denaturation [8, 9], population biology [10, 11], and molecular motors [find refs for conservative molecular motors]. In all these cases the dynamics can be regarded as a stochastic process in which a particle hops from site to site. The rate equation can be written in matrix notation as

$$\frac{d\boldsymbol{p}}{dt} \;=\; \boldsymbol{W}\boldsymbol{p}, \tag{1}$$

involving an $N \times N$ matrix $\boldsymbol{W}$ whose off-diagonal elements are the transitions rates w_{nm}, and with diagonal elements $-\gamma_n$ such that each column sums to zero. In the case of a one-dimensional ring-shaped lattice with near-neighbor hopping

$$\boldsymbol{W} \;=\; \begin{bmatrix} -\gamma_1 & w_{1,2} & 0 & ... \\ w_{2,1} & -\gamma_2 & w_{2,3} & ... \\ 0 & w_{3,2} & -\gamma_3 & ... \\ ... & ... & ... & ... \end{bmatrix} \tag{2}$$

In Einstein's theory $\boldsymbol{W}$ is symmetric, and all the non-zero rates are the same; In the resistor-network problem the rates have some distribution $P(w)$ that features

$$P(w) \;\propto\; w^{\alpha-1} \quad \text{(for small } w\text{)} \tag{3}$$

But in Sinai's problem $\boldsymbol{W}$ is allowed to be asymmetric. Accordingly the rates at the nth bond can be written as $w_n e^{\pm \mathscr{E}_n/2}$

for clockwise and anticlockwise transitions respectively. For the purpose of presentation we assume that the stochastic field $\mathscr{E}$ is box distributed within $[s - \sigma, s + \sigma]$.

Scope.– In this article we report how the spectral properties of the matrix $\boldsymbol{W}$ depend on the parameters (α, σ, s). These parameters describe respectively the resistor-network disorder, the stochastic-field disorder, and the average bias field. The eigenvalues $\{-\lambda_k\}$ of $\boldsymbol{W}$ are associated with the relaxation modes of the system. Due to conservation of probability $\lambda_0 = 0$, while all the other eigenvalues $\{\lambda_k\}$ have positive real part, and may have an imaginary part as well. Complex eigenvalues imply that the relaxation is not over-damped: one would be able to observe an oscillating density during relaxation, as demonstrated in Fig.1. The second row of Fig.2 provides some representative spectra. As the bias s is increased a complex bubble appears at the bottom of the band, implying delocalization of the eigenstates. Our results for the complexity threshold s_c are summarized in table I, and demonstrated in Fig.5. The number of complex eigenvalues grows as a function of the bias, as demonstrated in Fig.4, but asymptotically only a finite fraction of the spectrum becomes complex. Our objective below is to explain analytically the peculiarities of this delocalization transition, to explain how it is affected by the percolation and by the sliding thresholds, and to analyze the complexity-saturation effect.

Stochastic spreading.– We first consider an opened ring, namely a disordered chain. The asymmetry can be gauged away, and $\boldsymbol{W}$ becomes similar to a symmetric matrix $\boldsymbol{H}$. The statistics of its off-diagonal elements is characterized by α, while the statistics of the diagonal elements is also affected by σ and s. The eigenvalues $-\epsilon_k$ are real, and results for their spectral density are known. In the absence of disorder they form a band $[\epsilon_s, \epsilon_\infty]$ where $\epsilon_{s,\infty} = 2[\cosh(s/2) \mp 1]$. For sparse disorder with M ($\ll N$) disordered bonds, a few additional isolated eigenvalues might appear in the gap $[0, \epsilon_s]$. With full disorder it is possible to get a gapless spectrum. This is the case for Gaussian white-noise stochastic-field disorder as analyzed in [6]. In this case there is an analytical expression for the spectral density in terms of Bessel functions. The expression features

$$\rho(\epsilon) \;\propto\; \epsilon^{\mu-1} \quad \text{(for small } \epsilon\text{)} \tag{4}$$

with no gap. The exponent is related to the bias via $s = (1/2)\sigma^2 \mu$. In the present work we assume the more physically appealing log-box disorder for which (see Methods)

$$s \;=\; s_\mu \;=\; \frac{1}{\mu} \ln\left(\frac{\sinh(\sigma\mu)}{\sigma\mu} \right) \tag{5}$$

Unlike Gaussian disorder the range of possible rates is bounded, and we see that a finite threshold $s_\infty = \sigma$ is deduced. For $s > s_\infty$ a gap opens up. Using the above spectral properties

Type of disorder	Parameters	s_c	Remarks	Figure
Resistor-network disorder	$\alpha<\frac{1}{2}$, $\sigma=0$	$s_c=\infty$	non-percolating	Fig.5b
Resistor-network disorder	$\frac{1}{2}<\alpha<1$, $\sigma=0$	$s_c\sim(1/N)$	residual percolation	Fig.5b
Sparse disorder	$(M/N)\ll1$	$s_c\sim(1/N)$	both disorder types	Fig.5a
Stochastic field disorder	$\alpha>1$, $\sigma\neq0$	$s_c\approx s_{1/2}$	percolating	Fig.4

TABLE I: **The complexity threshold for different types of disorder**. (Aka delocalization transition). We distinguish between resistor network disorder and stochastic field disorder. The threshold $s_{1/2}$ reflects the strength σ of the latter. It is smaller than the s_1 threshold of the sliding transition. Note that the thresholds s_μ depend neither on N nor on α.
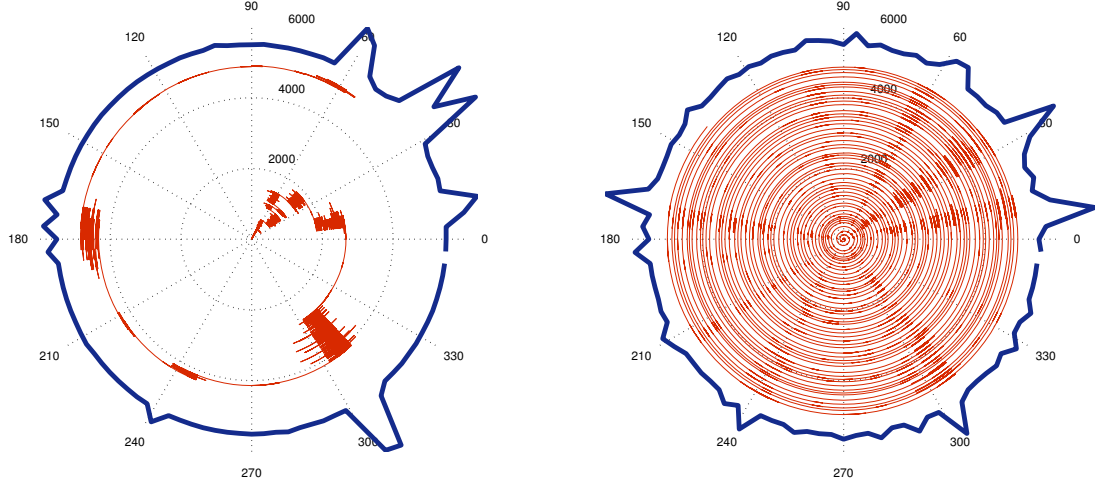

FIG. 1: **Simulated trajectory of a particle on a disordered-ring.** The number of sites is $N=100$ and the disorder strength is $\sigma=5$. The radial direction is time and the angle is the position. For small s (left panel $s=0.88$) the dynamics is over-damped, while for large s (right panel $s=2.97$) the dynamics is under-damped. The outer thick line is the steady-state distribution (see Methods).

it is deduced that the spreading of a distribution along an infinite chain goes like $x\sim t^\mu$ for $s<s_1$, while for $s>s_1$ we have a non-zero drift velocity. This is known as the "sliding transition". As for the second moment, for $\mu<1/2$ the diffusion coefficient is zero.

The introduction of resistor-network-disorder modifies the spectral density at higher energies. For $\alpha>1$, in the absence of bias, the continuum-limit approximation features $\mu=1/2$. This reflects a normal diffusive behavior as in Einstein's theory of Brownian motion. Below the percolation threshold, namely for $\alpha<1$, normal diffusion is suppressed, and the spectral exponent is $\mu=\alpha/(1+\alpha)<1/2$. But for large bias, the diagonal disorder in $\boldsymbol{H}$ dominates, leading to trivially localized eigenstates. Hence for large bias we simply have $\mu=\alpha$ irrespective of the percolation aspect.

Relaxation.– We close an N-site chain into a ring. The ring is characterized by its so-called affinity,

$$S_\circlearrowleft \equiv Ns \qquad (6)$$

Now a topological aspect is added to the problem, and one wonders what are the relaxation modes of the system. The starting point of our analysis is the secular equation for the eigenvalues of $\boldsymbol{W}$. Assuming that we already know what are the eigenvalues of the associated symmetric matrix $\boldsymbol{H}$, the

secular equation takes the form [12]

$$\prod_k\left(\frac{z+\epsilon_k(s)}{\overline{w}}\right) = 2\left[\cosh\left(\frac{S_\circlearrowleft}{2}\right)-1\right] \qquad (7)$$

where $\overline{w}$ is the geometric average of all the rates. The bias s affects both the ϵ_k and the right hand side. This equation has been analyzed in [13] in the case of a non-conservative matrix $\boldsymbol{W}$ whose diagonal elements γ_n are *fixed*, hence the $\epsilon_k(s)$ there do not depend on s. Consequently, as s of equation(6)) is increased beyond a threshold value s_c, the eigenvalues in the middle of the spectrum become complex. As s is further increased beyond some higher threshold value, the entire spectrum becomes complex. As already stated in the introduction, this is not the scenario that is observed for our conservative model. Furthermore we want to clarify how the percolation and sliding thresholds are reflected.

Already at this stage one should be aware of the immediate implications of conservativity. First of all $z=\lambda_0=0$ should be a root of the secular equation. The associated eigenstate is the non-equilibrium steady state (NESS), which is an extended state. In fact it follows that the localization length has to diverge as $\lambda\to0$. This is in essence the difference between the conventional Anderson model (Lifshitz tails at the band floor) and the Debye model (phonons at the band floor). It is the latter picture that applies in the case of a conservative model.
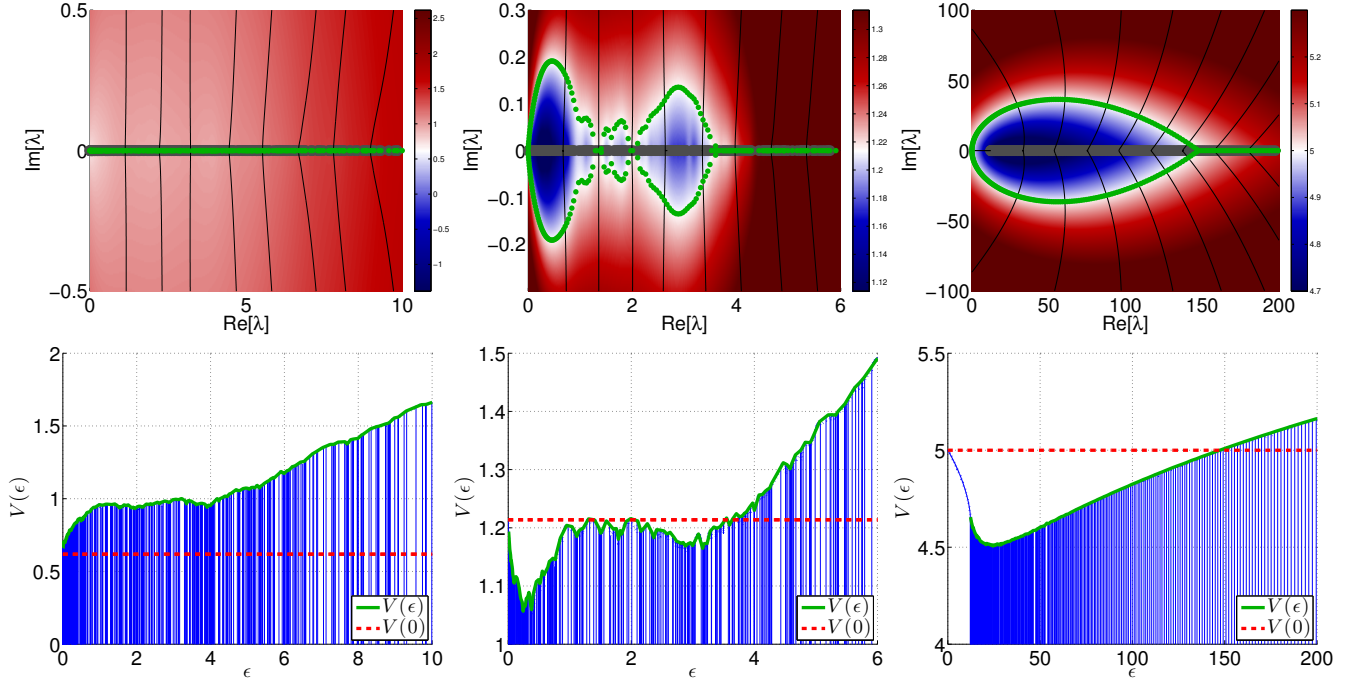
FIG. 2: **The emergence of complexity in the relaxation spectrum.** The upper panels display representative examples of relaxation spectra. The $\{\lambda_k\}$ are indicated by green points in the complex plane. The ring has $N=500$ sites with $\sigma=5$, and (from left to right) $s = 1.24, 2.43, 10$. The calculated threshold values are $s_{1/2} = 1.77$ and $s_1 = 2.7$ and $s_\infty = 5$. In the left hand column $s < s_{1/2}$ and the spectrum is real. In the middle column $s_{1/2} < s < s_\infty$ and the spectrum is with several complex bubbles separated by real segments. In the right column $s > s_\infty$ and the real spectrum has a gap, while the complex spectrum is a fully developed complex bubble, tangent to the origin (no gap). The "electrostatic field" that is associated with the secular equation is represented by a few field-lines, while the background color provides visualization of the corresponding potential. The spectrum is obtained by looking for the intersections of the field lines with the equipotential line $V(z) = V(0)$ that goes through the origin (indicated in white). The lower panels plot the potential $V(\epsilon)$ along the real axis. The horizontal dashed line is $V(0)$.

Electrostatic picture.– In order to get an insight into the secular equation we define an "electrostatic" potential by taking the log of the left hand side of equation (7). Namely,

$$\Psi(z) = \sum_k \ln(z - \epsilon_k) \equiv V(x, y) + iA(x, y) \qquad (8)$$

where $z = x + iy$. Note that we have flipped the sign convention ($z \mapsto -z$), and also we set the time units such that $\overline{w} = 1$. The constant $V(x, y)$ curves correspond to potential contours, and the constant $A(x, y)$ curves corresponds to stream lines. The derivative $\Psi'(z)$ corresponds to the field, which can be regarded as either electric or magnetic field up to a 90deg rotation. Using this language, the secular equation takes the form

$$V(x, y) = V(0); \quad A(x, y) = 2\pi * \text{integer} \qquad (9)$$

Namely the roots are the intersection of the field lines with the potential contour that goes through the origin. We want to find what are the conditions for getting a real spectrum from equation (9), and in particular what is the threshold s_c for getting complex eigenvalues at the bottom of the spectrum. We first look on the potential along the real axis:

$$V(\epsilon) = \int \ln(|\epsilon - x'|)\rho(x')dx' \qquad (10)$$

In regions where the $\{\epsilon_k\}$ form a quasi-continuum, one can identify $(1/N)V(\epsilon)$ as the Thouless expression for the inverse localization length [13]. The explicit value of $V(0)$ is implied by equation (7). For a charge-density that is given by equation (4), with some cutoff ϵ_c, the derivative of the electrostatic potential at the origin is (see Methods)

$$V'(\epsilon) \approx \frac{\epsilon^{\mu-1}}{\epsilon_c^\mu}\pi\mu\cot(\pi\mu) \qquad (11)$$

One observes that the sign changes from positive to negative at $\mu = 1/2$. Some examples are illustrated in Fig.2. Clearly, if the envelope of $V(\epsilon)$ is above the $V = V(0)$ line, then the spectrum is real, and the λ_k are roughly the same as the ϵ_k, shifted a bit to the left.

From the above it follows that the threshold s_c for the appearance of a complex quasi-continuum is either $V(\epsilon_s) < V(0)$ or $V'(0) < 0$, depending on whether $\rho(\epsilon)$ is gapped or not. In the latter case it follows from equation (11) that $s_c = s_{1/2}$. We note that for the Gaussian model of [6] one obtains $V(\epsilon \to \infty) = \text{const}$, implying that the entire spectrum would go from real to complex at $s = s_{1/2}$. In general this is not the case: the complex spectrum typically forms a "bubble" tangent to the origin, or possibly one may find some additional bubbles as in Fig.2b.
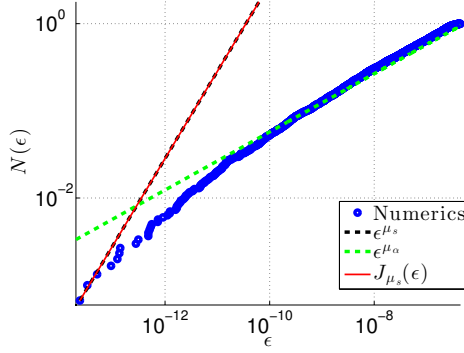
FIG. 3: **The spectrum of the associated hermitian matrix.** We calculate numerically the integrated density, which counts the eigenvalues $\{\epsilon_k < \epsilon\}$ of H for a ring with N=3000 sites. The system is characterized by a percolation exponent $\mu = \mu_\alpha = 1/3$, and by a scaled affinity $\mu = \mu_s = 1$. The stochastic-field distribution is with σ=2. The blue points are are results of numerical diagonalization. There is a crossover from density that corresponds to μ_s (dashed black line), to density that corresponds to μ_α (dashed green line). The red line is the Bessel expression of [6].

The identification of the s_c with $s_{1/2}$ holds for full disorder, but not for sparse disorder. In the latter case $s_c \propto 1/N$, or we may better look on $S_c = Ns_c$. The reasoning that leads to this conclusion is as follows: We start with a clean ring. Recall that $\rho(\epsilon)$ feature a gap $[0, \epsilon_s]$. If we have M defected bonds with some σ disorder the condition $V(\epsilon_s) < V(0)$ implies $S_c = M\sigma$ (see methods). The handling of weak links is a bit more complicated (see Methods) but leads to the same conclusion, where the role of σ is played by the dispersion of the defected w_n.

Complexity saturation.– The secular equation for the eigenvalues is given by equation (7). In the nonconservative case, the eigenvalues of H do not depend on s, thus raising s will eventually make the entire spectrum complex. For a conservative matrix, however, $V(\epsilon)$ is also a function of s, so increasing s raises $V(\epsilon)$ at the same rate. Taking s to be as large as desired, the eigenvalues of H become trivially $\gamma_n e^{\mathscr{E}_n/2}$, and the equation $V(\epsilon) = V(0)$ for the upper cutoff ϵ_c of the complex energies takes the form

$$\overline{\ln\left[\epsilon - w e^{\mathscr{E}/2}\right]} \;=\; s/2 \tag{12}$$

It is natural to write the stochastic field as $\mathscr{E} = s + \varsigma$, such that $\varsigma \in [-\sigma, +\sigma]$. For the purpose of presentation we assume that w=1. Then the spectrum stretches from $\epsilon_s = e^{(s-\sigma)/2}$ to $\epsilon_c = e^{(s+\sigma_c)/2}$, where σ_c is the solution of

$$\int_{-\sigma}^{\sigma} \ln\left|e^{\varsigma/2} - e^{\sigma_c/2}\right| d\varsigma \;=\; 0 \tag{13}$$

It follows that the fraction of complex eigenvalues is

$$\text{fraction} = \frac{1}{N}\int_{\epsilon_s}^{\epsilon_c} \rho(\epsilon) d\epsilon = \frac{1}{\sigma}\ln\left(\frac{\epsilon_c}{\epsilon_s}\right) = \frac{\sigma_c + \sigma}{2\sigma} \tag{14}$$

We demonstrate the agreement with this formula in Fig.4. We plot there also what happens if resistor-network disorder is
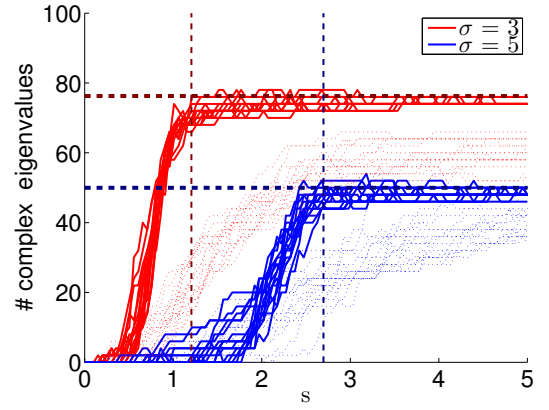

FIG. 4: **Complexity saturation.** The number of complex eigenvalues is counted for a ring with N=100 sites, for various values of the affinity s. Each red line corresponds to a different realization of field disorder with σ=3 (red) and σ=5 (blue). The vertical lines are the corresponding values of s_1, at which the sliding transition occurs. We see that the asymptotic fraction of complex eigenvalues saturates. The horizontal dashed line are the analytical estimates of equation (14). If the lattice were continuous with Gaussian disorder, the number of complex eigenvalues would go to 100%. In the background an $\alpha = 0.9$ resistor-network disorder is shown. The crossover is blurred and the saturation value is lower compared to equation (14).

introduced. We see that for small α the crossover is not as sharp and the saturation value is lower than equation (14) as expected from equation (12).

In conclusion.– we have shown that the spectral scenario that characterizes a biased conservative dynamics that is generated by a rate-equation in a closed circuit (or "chemical cycle" in the context of molecular motors) is dramatically different from that of a biased non-hermitian Hamiltonian. The transition to complexity depends on the type of disorder as summarized in table I. Surprisingly it happens for $\alpha > 1/2$ before the percolation transition, and for $\mu > 1/2$ before the sliding transition, and diminishes as $1/N$ for sparse disorder. Further increasing the bias does not lead to full delocalization, instead a "complexity saturation" is observed.

I. METHODS

The NESS formula.– Following the derivation in [14] the explicit formula for the NESS is

$$p_n \propto \left(\frac{1}{w_{\overrightarrow{n}}}\right)_s e^{-(U(n) - U_s(n))} \tag{15}$$

where $U(n)$ is the stochastic potential that associated with the field $\mathscr{E}_n$, the transitions in the drift-wise direction are $w_{\overrightarrow{n}} = w_n e^{\mathscr{E}_n/2}$, and the subscript s indicates drift-wise smoothing over a length scale $1/s$. Note that in the absence of bias the smoothed functions are constant and we get the canonical equilibrium state.

Finding s_μ.– The cummulant generating function of the stochastic field can be written as $g(\mu) = (s - s_\mu)\mu$, where the
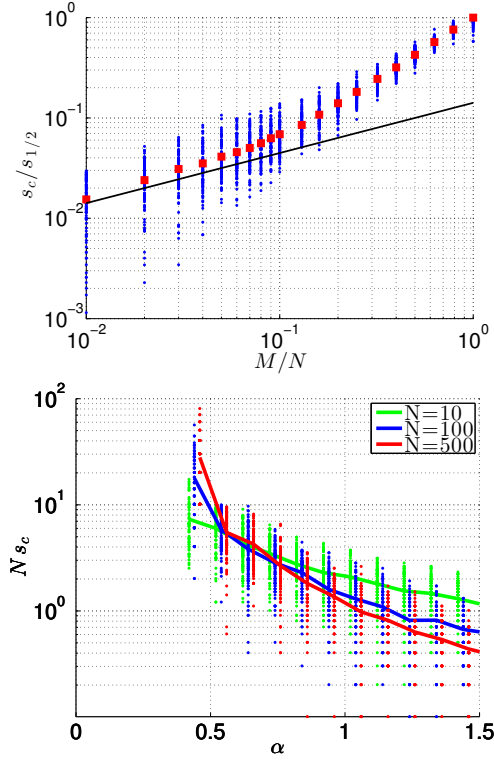
FIG. 5: **The complexity threshold.** Top panel: The threshold value s_c for delocalization versus the number of stochastic field defects M. The number of sites is $N=100$ and the disorder strength (of the defected sites) is $\sigma=5$. Blue dots correspond to different realizations, while red dots are the average (per M). For a fully disordered lattice we expect $s_c = s_{1/2}$, hence the scaling of the axes. The black line is $S_c = M\sigma$. bottom panel: The threshold value s_c versus α. The dots are for different realizations, while the lines are the statistical average. For $\alpha < 1/2$ the s_c diverges as N is increased. Data points for each N are slightly shifted for clarity.

s_μ are defined via the following expression:

$$\left\langle e^{-\mathscr{E}\mu} \right\rangle \equiv e^{-(s-s_\mu)\mu} \tag{16}$$

If the stochastic field has normal distribution with standard deviation σ, then $s_\mu = (1/2)\sigma^2\mu$. For our log-box distribution equation (5) applies. The finite value of s_∞ reflects that $\mathscr{E}$ is bounded.

Finding $V'(0)$.– To derive equation (11) we assume an integrated density of states that corresponds to equation (4), namely, $\mathscr{N}(\epsilon) = (\epsilon/\epsilon_c)^\mu$, where ϵ_c is some cutoff that reflects the discreteness of the lattice. After integration by parts the electrostatic potential along the real axis is given by

$$V(\epsilon) = -\int_0^{\epsilon_c} \frac{\mathscr{N}(x)}{x-\epsilon}dx \tag{17}$$

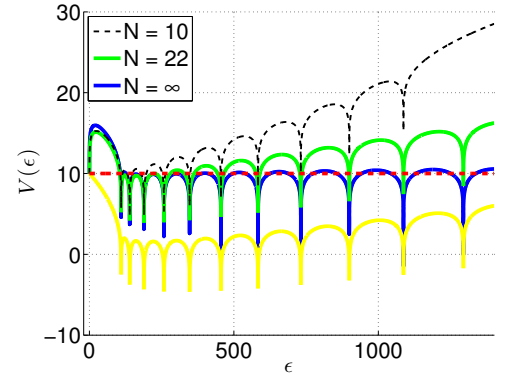While calculating the derivative we assume $\epsilon \ll \epsilon_c$, hence tak-

FIG. 6: **Graphical illustration of the the secular equation for a ring with a weak link.** The red line is $V(0) = \ln[2(\cosh(S_\circlearrowright/2) - 1)]$. The blue line is $V(\epsilon)$ as deduced from the LHS of equation (22) with $L = 1$ and $g = 10^{-3}$ and $S_\circlearrowright = 20$ check. The yellow line is an attempted reconstruction of $V(\epsilon)$ from the first $N = 22$ roots ϵ_k of the $S_\circlearrowright=0$ equation. The green line is a proper reconstruction that takes into account an impurity term ϵ_0. The deviation from the blue line for large k is due to finite truncation: compare the $N=10$ line with the $N=22$ line.

ing the upper limit of the scaled integral as infinity:

$$V'(\epsilon) = \frac{\mu}{\epsilon_c^\mu}\epsilon^{\mu-1}\int_0^\infty \frac{z^{\mu-1}}{z-1}dz \tag{18}$$

$$= -\frac{\mu}{\epsilon_c^\mu}\epsilon^{\mu-1} B_\infty(\mu,0) \tag{19}$$

where $B_u(a,b)$ is the Incomplete Euler Beta function. Taking the Cauchy principal part we get

$$B_\infty(\mu,0) = \lim_{\delta\to 0}[B_{1-\delta}(\mu,0) - B_{1-\delta}(1-\mu,0)] \tag{20}$$

$$= \psi(1-\mu) - \psi(\mu) = \pi\cot(\pi\mu) \tag{21}$$

where $\psi(z)$ is the digamma function, and the last equality has been obtained by the reflection formula.

Finding s_c due to a biased-link.– We consider a clean ring. We assume that the stochastic field over one bond is exceptionally large compared to all other bonds. Then there is an extra "impurity" level $\epsilon_1 \approx \gamma_1 \approx \exp[(s+\sigma)/2]$ that is located above the continuum of extended modes. The contribution of this impurity to $V(\epsilon_s)$ is $\ln(\epsilon_s - \gamma_1)$. The contribution of the continuum can be neglected due to the Thouless relation. Hence the condition $V(\epsilon_s) > V(0)$ implies $s_c \approx \sigma/N$.

Finding s_c due to a weak-link.– We consider a clean ring of length $L = Na$ with identical bonds ($w_n = 1$). We change one bond into a weak link ($w_1 \ll 1$). This setup can be treated exactly in the continuum limit, where equation (1) corresponds to a diffusion equation with coefficient $D_0 = wa^2$ and drift velocity $v_0 = swa$. The weak link corresponds to a segment where the diffusion coefficient is $D_1 \ll D_0$. Using transfer

matrix methods we find the secular equation

$$\cos(k) + \frac{1}{g}\frac{k^2 + \left(\frac{S_\circlearrowleft}{2}\right)^2}{2k}\sin(k) \;=\; \cosh\left(\frac{S_\circlearrowleft}{2}\right) \qquad (22)$$

where $k^2 = (L^2/D)z - (S_\circlearrowleft/2)^2$, and $g = (D_1/a)/(D_0/L)$. We have taken here the limit $a \to 0$, keeping $(L, g, S_\circlearrowleft)$ constant. The equation is graphically illustrated in Fig.6. All the roots are real solutions provided the envelope of the left-hand-side (LHS) lays above the right-hand-side. The minimum of the envelope of the LHS is obtained at $z = S_\circlearrowleft^2/2$. Consequently we find that the threshold S_c obeys

$$\frac{S_\circlearrowleft}{2g} \;=\; \cosh\left[\frac{S_\circlearrowleft}{2}\right] \qquad (23)$$

provided $S_\circlearrowleft \gg g$, which is self-justified for small g. The solution is given in terms of the Lambert function, namely $S_c = -2\mathrm{W}(-g/2)$, leading to $s_c = S_c/N$.

The secular, equation equation (22), parallels the discrete version equation (7), with a small twist that we would like to point out. Naively one would like to identify $\ln[2(\mathrm{LHS} - 1)]$, up to a constant, with $\sum_{k=1}^{\infty} \ln(\epsilon - \epsilon_k)$, where the the the ϵ_k are the $S_\circlearrowleft{=}0$ roots of equation (22). This is tested in Fig.6, and we see that there is a problem. Then one realizes that in fact an additional $k = 0$ term with $0 \lesssim \epsilon_0 < \epsilon_s$ is missing. Going back to the discrete version it corresponds to an impurity-level that is associated with a mode which is located at the weak-link. While taking the limit $a \to 0$ this level becomes excluded. Adding it back we we see that the agreement between equation (7) and equation (22) is restored. The residual systematic error as k becomes larger is due to finite truncation. Making the approximation $\ln(\epsilon_s - \epsilon_0) \approx \ln[(s/2)^2]$, and noting that $g \propto N$, it is verified that the equation $V(\epsilon_s) = V(0)$ for the complexity threshold is consistent with equation (23).

[1] S. Alexander, J. Bernasconi, W. R. Schneider, and R. Orbach, Rev. Mod. Phys. **53**, 175 (1981), URL http://link.aps.org/doi/10.1103/RevModPhys.53.175.

[2] A. Vaknin, Z. Ovadyahu, and M. Pollak, Phys. Rev. Lett. **84**, 3402 (2000), URL http://link.aps.org/doi/10.1103/PhysRevLett.84.3402.

[3] A. Amir, Y. Oreg, and Y. Imry, Phys. Rev. Lett. **103**, 126403 (2009), URL http://link.aps.org/doi/10.1103/PhysRevLett.103.126403.

[4] Y. G. Sinai, Theory of Probability & Its Applications **27**, 256 (1983), http://dx.doi.org/10.1137/1127028, URL http://dx.doi.org/10.1137/1127028.

[5] B. Derrida, Journal of Statistical Physics **31**, 433 (1983), ISSN 0022-4715, URL http://dx.doi.org/10.1007/BF01019492.

[6] J. Bouchaud, A. Comtet, A. Georges, and P. L. Doussal, Annals of Physics **201**, 285 (1990), ISSN 0003-4916, URL http://www.sciencedirect.com/science/article/pii/000349169090043N.

[7] J.-P. Bouchaud and A. Georges, Physics Reports **195**, 127 (1990), ISSN 0370-1573, URL http://www.sciencedirect.com/science/article/pii/037015739090099N.

[8] D. K. Lubensky and D. R. Nelson, Phys. Rev. Lett. **85**, 1572 (2000), URL http://link.aps.org/doi/10.1103/PhysRevLett.85.1572.

[9] D. K. Lubensky and D. R. Nelson, Phys. Rev. E **65**, 031917 (2002), URL http://link.aps.org/doi/10.1103/PhysRevE.65.031917.

[10] D. R. Nelson and N. M. Shnerb, Phys. Rev. E **58**, 1383 (1998), URL http://link.aps.org/doi/10.1103/PhysRevE.58.1383.

[11] K. A. Dahmen, D. R. Nelson, and N. M. Shnerb, in *Statistical mechanics of biocomplexity* (Springer, 1999), pp. 124–151.

[12] L. G. Molinari, Linear Algebra and its Applications **429**, 2221 (2008), ISSN 0024-3795, URL http://www.sciencedirect.com/science/article/pii/S0024379508003200.

[13] N. M. Shnerb and D. R. Nelson, Phys. Rev. Lett. **80**, 5172 (1998), URL http://link.aps.org/doi/10.1103/PhysRevLett.80.5172.

[14] D. Hurowitz and D. Cohen, Phys. Rev. E **90**, 032129 (2014), URL http://link.aps.org/doi/10.1103/PhysRevE.90.032129.